Theory of reduced built-in polarization field in nitride-based quantum dots

S. Schulz[1] and E. P. O'Reilly[1,2]
[1]*Tyndall National Institute, Lee Maltings, Cork, Ireland*
[2]*Department of Physics, University College Cork, Cork, Ireland*
(Received 26 March 2010; published 27 July 2010)

We use a surface integral method to show that the polarization potential in an InGaN/GaN quantum dot (QD) grown along the [0001] direction is strongly reduced compared to that in a quantum well (QW) of the same height. We use simple analytic expressions and different dot geometries to show that the reduction originates from two effects (i) the reduction in the QD [0001] surface area and (ii) strain redistributions in the QD system. The In composition can therefore be increased in a QD compared to a QW, enabling efficient recombination to longer wavelengths in InGaN QD structures.

DOI: 10.1103/PhysRevB.82.033411 PACS number(s): 68.65.Hb, 73.22.Dj, 77.22.Ej, 77.65.Ly

Nitride-based semiconductor materials InN, GaN, AlN, and their alloys attract great attention due to their promising applications in optoelectronic devices such as light-emitting devices (LEDs) and laser diodes.[1] Depending on the alloy composition, these systems are, in principle, able to cover a wide wavelength range from blue through green and yellow to red.[2] Especially for energy-efficient solid state lighting, which combines output from blue, green, and red LEDs, InGaN systems are promising candidates, because the assistance of phosphor is not required for a white light source. However, the emission efficiency of *c*-plane InGaN/GaN QWs drops significantly when going to longer wavelengths through use of higher In composition or thicker QWs. This behavior is attributed to the strong electrostatic built-in fields in nitride-based heterostructures grown along the polar [0001] direction.[3] These intrinsic fields arise in part from the spontaneous and in part from the piezoelectric polarization and lead to a strong spatial separation of electron and hole wave functions and therefore reduced radiative recombination rates.[4,5] Due to the large lattice mismatch between InN and GaN ($\approx$11%), a higher In concentration increases the strain-related piezoelectric part of the built-in potential, limiting the ability to go to longer wavelengths.

There is therefore considerable interest in ways to reduce the built-in polarization potential in InGaN structures.[6] We show and explain here why there is significant benefit in terms of field reduction when going from a *c*-plane QW to a *c*-plane quantum dot (QD) structure. Such an effect has been observed in recent work of Wu *et al.*[7] who used a self-consistent model based on atomistic strain field calculations and $\mathbf{k}\cdot\mathbf{p}$ theory to systematically study the electronic and optical properties of InGaN QD and QW systems. Their work showed that the QD systems can provide better electron-hole wave function overlap and therefore faster radiative recombination rates. However this gives rise to several questions. What is the reason for the reduction in the built-in field in QDs compared to QW structures? Is this reduction in the intrinsic built-in field a particular feature of the chosen QD geometry? Can the reduction in the built-in field in a QD allow a considerably increased In content in the QD compared to a QW of the same height?

To answer these questions and to achieve a realistic description of the polarization potential in nitride-based nanostructures we apply here a real-space surface integral approach developed by Williams *et al.*[8] This method admits analytic solutions in certain cases and provides an extremely useful insight into the parameters that influence the magnitude and the shape of the potential.

The total built-in polarization $\mathbf{P}^{\mathrm{tot}}$ in a nitride-based nanostructure with a wurtzite crystal structure is given by $\mathbf{P}^{\mathrm{tot}}=\mathbf{P}^{\mathrm{str}}+\mathbf{P}^{\mathrm{sp}}$. The first contribution $\mathbf{P}^{\mathrm{str}}$ refers to the strain-induced piezoelectric polarization while the second term $\mathbf{P}^{\mathrm{sp}}$ denotes the spontaneous polarization which arises from the lack of inversion symmetry along the *c* axis in a wurtzite lattice. Because of the crystal symmetry the vector $\mathbf{P}^{\mathrm{sp}}$ is oriented along the *c* direction. The corresponding potential ϕ_{sp} in a heterostructure then arises due to the difference at the interface, $\Delta\mathbf{P}^{\mathrm{sp}}=\mathbf{P}^{\mathrm{sp}}_{\mathrm{NS}}-\mathbf{P}^{\mathrm{sp}}_{\mathrm{B}}$, between the nanostructure, $\mathbf{P}^{\mathrm{sp}}_{\mathrm{NS}}$, and the barrier, $\mathbf{P}^{\mathrm{sp}}_{\mathrm{B}}$, spontaneous polarization vector. The potential ϕ_{sp} is then given by an integral over the QD surfaces normal to the [0001] direction.[8]

The second contribution to the built-in potential stems from the piezoelectric polarization $\mathbf{P}^{\mathrm{str}}$, which depends on the local strain as[8]

$$\mathbf{P}^{\mathrm{str}}=\begin{pmatrix}2e_{15}\epsilon_{xz}\\ 2e_{15}\epsilon_{yz}\\ e_{31}(\epsilon_{xx}+\epsilon_{yy})+e_{33}\epsilon_{zz}\end{pmatrix}=\begin{pmatrix}P_x^{\mathrm{shear}}\\ P_y^{\mathrm{shear}}\\ P^{\mathrm{axial}}\end{pmatrix}. \quad (1)$$

The different piezoelectric constants and strain components are denoted by e_{ij} and ϵ_{ij}, respectively. In contrast to a QW structure, where the shear strain components are zero, the polarization vector $\mathbf{P}^{\mathrm{str}}$ in Eq. (1) can have nonzero components in all three directions in a QD. Furthermore, and contrary to the spontaneous polarization $\mathbf{P}^{\mathrm{sp}}$, $\mathbf{P}^{\mathrm{str}}$ is not a constant vector within the QD, since the strain field is position dependent. By using integral expressions for the strain field, in combination with Maxwell's equations, it is possible to derive the three-dimensional piezoelectric polarization potential $\phi_{\mathrm{str}}(\mathbf{r})$ by evaluating two two-dimensional integrals over the [0001]-oriented surface of the QD. A detailed description of the applied approach is given in Ref. 8.

Before we discuss realistic QD geometries, let us start with a simple system to illustrate how the built-in potential evolves in going from a *c*-plane QW to a *c*-plane QD of the same height. Therefore, we consider here in a first step the built-in potential in a cuboid-shaped QD. A complete ana-

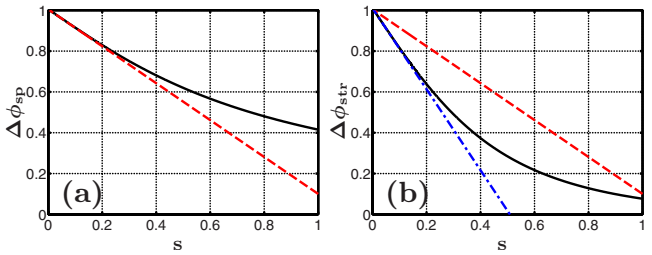

FIG. 1. (Color online) (a) Normalized variation of the potential drop in the spontaneous potential $\Delta\phi_{sp}$ across a cuboid-shaped QD as a function of the height to base length ratio $s=h/B$. Solid line shows $\Delta\phi_{sp}$ using the exact solution from Ref. 8; dashed (red) line is calculated using Eq. (2). (b) Solid line, normalized variation in the strain-related piezoelectric potential $\Delta\phi_{str}$ using exact solution from Ref. 8. Dashed (red) and dashed-dotted (blue) lines, results from Eq. (3) assuming, respectively, constant strain only (first term), and allowing also for first-order changes in the strain field (both terms).

lytic solution of the integrals involved in the applied surface integral method can be obtained for this case.[8] We start with the contribution arising from the spontaneous polarization potential in a cuboid-shaped QD of height $2h$ and base length $2B$ centered at the origin. The potential difference $\Delta\phi_{sp}$ between the top and bottom center of the cuboid-shaped QD will be discussed in the following as a function of $s=h/B$, where $s=0$ corresponds to the QW limit.

From the analytic solution for the spontaneous polarization ϕ_{sp} given in Ref. 8, we obtain that the potential difference $\Delta\phi_{sp}$ varies between the top and the bottom surface of the cuboid for small s as

$$\Delta\phi_{sp} \approx \left[\frac{2(P_{QD}^{sp} - P_{B}^{sp})}{\varepsilon_0\varepsilon_r}\right] h\left(1 - \frac{2\sqrt{2}}{\pi}s\right). \tag{2}$$

This result shows that $\Delta\phi_{sp}$ decreases approximately linearly with s in a QD compared to a QW structure of the same height, as shown in Fig. 1(a). This is due to the reduction of the [0001] surface area of the QD and therefore to a reduction in the surface charge compared to the corresponding QW system.

The second contribution to the total built-in potential originates from the piezoelectric part, Eq. (1). The corresponding potential ϕ_{str} is modified by two factors when going from a QW to a QD of the same height. First, as in the case of the spontaneous polarization potential ϕ_{sp} the finite size of the QD affects the piezoelectric contribution. Second, there is also a strain redistribution in the QD compared to a QW. By using the equations given in Ref. 8, the potential difference $\Delta\phi_{str}$ between the top and the bottom surfaces of the QD varies for small s as

$$\Delta\phi_{str} \approx C_1 h\left(1 - \frac{2\sqrt{2}}{\pi}s\right) - C_2 h\frac{2\sqrt{2}}{\pi}s \tag{3}$$

with

$$C_1 = \frac{2\epsilon_0[2e_{31} + (1-A)e_{33}]}{\varepsilon_r\varepsilon_0} \tag{4}$$

and

$$C_2 = \frac{\epsilon_0 A[2e_{15} - e_{33} + e_{31}]}{\varepsilon_r\varepsilon_0}. \tag{5}$$

Here, ϵ_0 is the isotropic misfit strain, ε_r is the dielectric constant, and $A=\frac{1-\nu}{1+\nu}$ where ν denotes the Poisson ratio. The first term on the right-hand side (RHS) of Eq. (3) is of the same form as the result for the potential difference $\Delta\phi_{sp}$ arising from the spontaneous part given by Eq. (2). The second (C_2) term originates from the strain redistribution in the QD, including contributions from the shear strain part of the piezoelectric polarization (e_{15}) as well as axial terms related to e_{31} and e_{33}. In the case of a QW we have a biaxial compressive strain in the c plane and a tensile strain along the [0001] direction. Due to the finite size of the QD structure, this system is able to relax both in the x-y plane (c plane) and also along the [0001] direction so that the magnitude of each of the axial strain components is then reduced in the QD ($|\epsilon_{ii}^{QD}| \leq |\epsilon_{ii}^{QW}|$). The strain-related piezoelectric potential drop $\Delta\phi_{str}$ across the nanostructure is shown as a function of s in Fig. 1(b). The full calculation, based on the results given in Ref. 8, is shown by the solid line. The (red) dashed line is given by the first term on the RHS of Eq. (3) while the (blue) dashed-dotted line uses both terms on the RHS of Eq. (3). From Fig. 1(b) we see that the piezoelectric potential drop $\Delta\phi_{str}$ is reduced by approximately 60% for $s=0.4$ with approximately equal contributions to this reduction from the strain redistribution in the QD system and the reduction of the QD surface area compared to a QW.

So far we have discussed as a model system a cuboid-shaped QD. A similar analysis can also be undertaken for a cylindrical QD.[9] It should be noted that the potential drop in the cylindrical shaped QD, analyzed in Ref. 9, is studied in terms of $f=h/R$, where R is the radius and h the *total* height. We turn now to discuss the potential drop for more realistic QD shapes. For example, the experimental findings in Refs. 10 and 11 suggest an ellipsoid as the shape of InGaN QDs. Such a geometry was also used in a recent $\mathbf{k}\cdot\mathbf{p}$ calculation.[12] Again, using the results given in Ref. 8 for an ellipsoidal dot centered at the origin, with semimajor radius a and semiminor radius b, we calculate the potential drop across the nanostructure as a function of $s=b/a$.[13] The results for the calculated drop in the spontaneous potential $\Delta\phi_{sp}$ across the QD are shown in Fig. 2(a) while those for $\Delta\phi_{str}$ are shown in Fig. 2(b) with the approximate solutions for small s in both cases including terms up to s^3. Comparing the results to those for the cuboid-shaped QD [cf. Fig. 1(a)], we observe that the drop in the spontaneous potential difference $\Delta\phi_{sp}$ [cf. Fig. 2(a)] is clearly increased in the case of the ellipsoid-shaped dot. The same is true for the drop in the piezoelectric potential difference $\Delta\phi_{str}$, as shown in Figs. 1(b) and 2(b), respectively. This further reduction is directly due to the curved shape of the QD side walls. In a cuboid QD, each point in the dot is below all points on the full [0001]-oriented top surface so that all surface points then give contributions of the same

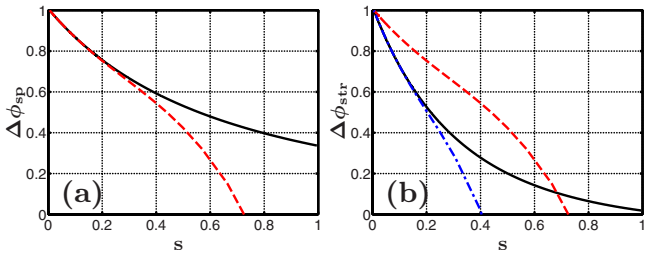

FIG. 2. (Color online) (a) Normalized variation in $\Delta\phi_{sp}$ across an ellipsoid shaped QD as a function of the semiminor to semimajor axis ratio $s=b/a$. Solid black line, exact solution from Ref. 8; dashed (red) line, cubic approximation for small s. (b) Normalized variation in $\Delta\phi_{str}$; solid line, exact solution from Ref. 8; dashed (red) line, results obtained by assuming constant strain; dashed-dotted (blue) line accounts for the finite QD size and changes in the strain field.

sign to the total potential. With a curved top surface, points near the top of the dot experience contributions of opposite sign from points on the upper surface of the dot which are below and above the given point, leading to an overall reduction in the total potential change.

A similar effect can be seen in Fig. 3, where we plot the normalized variation in the drop in the potential difference when going from a QW to a lens-shaped QD as a function of $s=h/D$, where h is the height of the lens and D the base diameter. Such a QD geometry is suggested by cross-sectional Z-contrast scanning transmission electron microscopy results.[14] By comparing the results of the lens-shaped system, the ellipsoidal QD and the cylindrical shaped dot[9] for the same aspect ratio (e.g., $s=0.5$; $f=1$), we conclude that $\Delta\phi$ is almost the same in the first two systems, while $\Delta\phi$ is considerably larger for the cylindrical QD. Again, this finding can be attributed to the vertical QD side walls in the case of the cylindrical-shaped dot.

Having analyzed the normalized variation of the potential when going from a QW to QD, we now consider the behavior of the total (spontaneous+piezoelectric) built-in potential ϕ^{tot} in specific InGaN/GaN QDs and QWs of the same height. We use the surface integral technique with a linear interpolation for all the material parameters,[15,16] except for

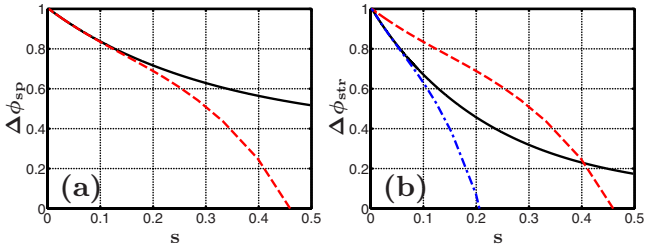

FIG. 3. (Color online) (a) Normalized variation in $\Delta\phi_{sp}$ across a lens-shaped QD of height h as a function of the height to diameter ratio $s=h/D$, where D is the diameter of the lens. Solid black line, exact solution from Ref. 8; dashed (red) line, cubic approximation for small s. (b) Normalized variation in $\Delta\phi_{str}$. Solid line, exact solution from Ref. 8; dashed (red) line, results obtained assuming constant strain; dashed-dotted (blue) line accounts both for the finite QD size and also for changes in the strain field.

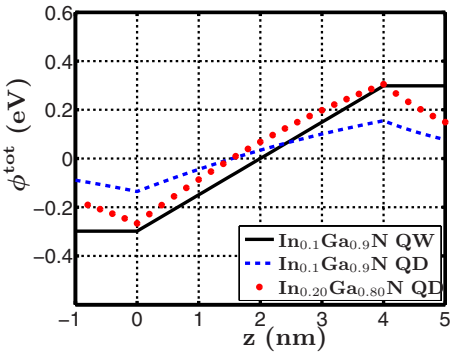

FIG. 4. (Color online) Total built-in potential ϕ^{tot} in an $In_{0.10}Ga_{0.90}N$ QW of height $h=4$ nm (solid line) in comparison to ϕ^{tot} of a lens-shaped $In_{0.10}Ga_{0.90}N$ and $In_{0.20}Ga_{0.80}N$ QD, respectively, with diameter $D=20$ nm and height $h=4$ nm.

the spontaneous polarization, where we apply a quadratic interpolation.[16] From the literature,[14,17,18] the average diameter of InGaN/GaN QDs scatters around 15–25 nm while the average height is approximately 2–5 nm. Here we assume a lens-shaped InGaN/GaN QD with diameter $d=20$ nm and height $h=4$ nm, which we compare with an $In_{0.10}Ga_{0.90}N$ QW of the same height. Our main focus here is on the general comparison of the built-in fields in QD and QW structures rather than describing the nanostructure in all details. Therefore, we neglect alloy fluctuations inside these low-dimensional systems. In the case of the $In_{0.10}Ga_{0.90}N/GaN$ QW, this assumption is in accordance with the experimental results given in Ref. 19. For a QD system the situation is more complicated. Here, alloy fluctuations inside the dot may lead to a situation where we do not have a sharp dot-barrier interface. Therefore, this might reduce the built-in potential even further compared to a situation with a sharp interface. Thus, the assumption of an homogeneously alloyed QD with sharp interfaces should provide a conservative estimate for the built-in field reduction in a QD compared to a QW of the same height.

The total built-in potential ϕ^{tot}, for a line scan through the QW is displayed in Fig. 4 (solid line). ϕ^{tot} shows a capacitorlike behavior. The potential for a line scan along the central axis of the corresponding lens-shaped $In_{0.10}Ga_{0.90}N$ QD is given by the (blue) dashed line. As expected from the analysis above, ϕ^{tot} is strongly decreased, by a factor of order 3, in the case of the QD compared to the QW. This result is supported by the experimental findings obtained by Grandjean *et al.* in Ref. 19. The experimental analysis in Ref. 19 shows that the radiative efficiency is strongly improved in $In_{0.15}Ga_{0.85}N/GaN$ QDs compared to $In_{0.10}Ga_{0.90}N$ QWs made from homogeneous ternary alloys. This effect can be related to carrier confinement effects and also to a reduction in the built-in field in a QD compared to a QW.

To obtain a potential difference between the upper and lower surface of the lens-shaped QD which is comparable to the potential difference of the $In_{0.10}Ga_{0.90}N$ QW the In content in the QD can be increased by a factor on the order of 2 (red dotted line) as shown in Fig. 4. Here, our analysis was carried out for a lens-shaped system. One peculiarity of the growth of InGaN/GaN QDs is the lack of control over the

geometrical features of these systems, at least compared to GaN/AlN QD structures. However, according to the detailed analysis of the influence of the QD geometry on the built-in field reduction in a QD, the calculated increase of In composition at fixed potential difference and dot height should also hold for different geometries. Another difficulty in the growth of $In_xGa_{1-x}N/GaN$ QD structures is the control of the In content in the QD system. Nevertheless, QD structures with 15–25 % In have been reported in the literature.[19–21] Thus, the QW and QD systems compared here are of experimental relevance.

In summary, we have presented a detailed comparison of the built-in potential in *c*-plane InGaN/GaN QWs and QDs with different geometries. Our analysis confirmed that the built-in field in an InGaN QD is strongly reduced compared to a QW of the same height. This reduction can be attributed to two effects: first, the reduction of the [0001] surface area in the QD compared to the QW and, second, the strain redistribution in the QD. Furthermore, from our comparison of the total built-in potential in a lens-shaped InGaN QD and a QW of the same height, we conclude that the In content in a dot can be increased considerably for a comparable field in both systems. This suggests that InGaN QDs are promising candidates to achieve efficient optical recombination at longer wavelength.

This work has been supported by Science Foundation Ireland. S.S. acknowledges further support from the Irish Research Council for Science, Engineering and Technology (IRCSET).

[1] S. C. Jain, M. Willander, J. Narayan, and R. V. Overstraeten, J. Appl. Phys. **87**, 965 (2000).
[2] C. J. Humphreys, MRS Bull. **33**, 459 (2008).
[3] J. Simon, N. T. Pelekanos, C. Adelmann, E. Martinez-Guerrero, R. Andre, B. Daudin, L. S. Dang, and H. Mariette, Phys. Rev. B **68**, 035312 (2003).
[4] A. D. Andreev and E. P. O'Reilly, Phys. Rev. B **62**, 15851 (2000).
[5] S. Schulz, S. Schumacher, and G. Czycholl, Phys. Rev. B **73**, 245327 (2006).
[6] T. Wunderer, F. Lipski, S. Schwaiger, J. Hertkorn, M. Wiedenmann, M. Feneberg, K. Thonke, and F. Scholz, Jpn. J. Appl. Phys. **48**, 060201 (2009).
[7] Y.-R. Wu, Y.-Y. Lin, H.-H. Huang, and J. Singh, J. Appl. Phys. **105**, 013117 (2009).
[8] D. P. Williams, A. D. Andreev, E. P. O'Reilly, and D. A. Faux, Phys. Rev. B **72**, 235318 (2005).
[9] D. P. Williams, S. Schulz, A. D. Andreev, and E. P. O'Reilly, IEEE J. Sel. Top. Quantum Electron. **15**, 1092 (2009).
[10] A. Strittmatter, L. Reißmann, R. Seguin, S. Rodt, A. Brostowski, U. Pohl, D. Bimberg, E. Hahn, and D. Gerthsen, J. Cryst. Growth **272**, 415 (2004).
[11] D. Gerthsen, E. Hahn, B. Neubauer, V. Potin, A. Rosenauer, and M. Schowalter, Phys. Status Solidi C **0**, 1668 (2003).
[12] M. Winkelnkemper, R. Seguin, S. Rodt, A. Hoffmann, and D. Bimberg, J. Phys.: Condens. Matter **20**, 454211 (2008).
[13] Please note that the term $\mp 2\pi\,\mathrm{sgn}(z\pm b)(z\pm b)\frac{a^2}{c^2}[\frac{3b^2}{c^2}+\frac{c^2-b^2+z(z\pm b)}{c^2+z^2}]$ is missing in Eq. (B13) for I_1 given in the Appendix of Ref. 8 for an ellipsoid-shaped system.
[14] M. Sénès, K. L. Smith, T. M. Smeeton, S. E. Hooper, and J. Heffernan, Phys. Rev. B **75**, 045314 (2007).
[15] K. Shimada, Jpn. J. Appl. Phys., Part 2 **45**, L358 (2006).
[16] I. Vurgaftman and J. R. Meyer, J. Appl. Phys. **94**, 3675 (2003).
[17] O. Moriwaki, T. Someya, K. Tachibana, S. Ishida, and Y. Arakawa, Appl. Phys. Lett. **76**, 2361 (2000).
[18] L. W. Ji, Y. K. Su, S. J. Chang, L. W. Wu, T. H. Fang, J. F. Chen, T. Y. Tsai, Q. K. Xue, and S. C. Chen, J. Cryst. Growth **249**, 144 (2003).
[19] N. Grandjean, B. Damilano, and J. Massies, IPAP Conf. Ser. **1**, 397 (2000).
[20] J. W. Robinson, J. H. Rice, K. H. Lee, J. H. Na, R. A. Taylor, D. G. Hasko, R. A. Oliver, M. J. Kappers, C. J. Humphreys, and G. A. D. Briggs, Appl. Phys. Lett. **86**, 213103 (2005).
[21] S.-K. Choi, J.-M. Jang, S.-H. Yin, J.-A. Kim, and W.-G. Jung, Proc. SPIE **6831**, 683119 (2007).